A new nonhydrostatic capability for MPAS-Ocean

Sara Calandrini, Darren Engwirda, Luke Van Roekel

PETSC USER MEETING 2023

June 5, 2023

Los Alamos
NATIONAL LABORATORY
EST.1943

LA-UR-23-25675

MPAS-Ocean component

The Model for Prediction Across Scales-Ocean (**MPAS-Ocean**) is an open-source, global ocean model and is one component within the Department of Energy's E3SM framework, which includes atmosphere, sea-ice, and land-ice models.

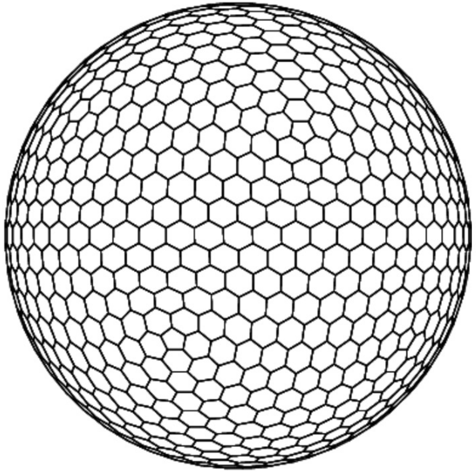

Horizontal

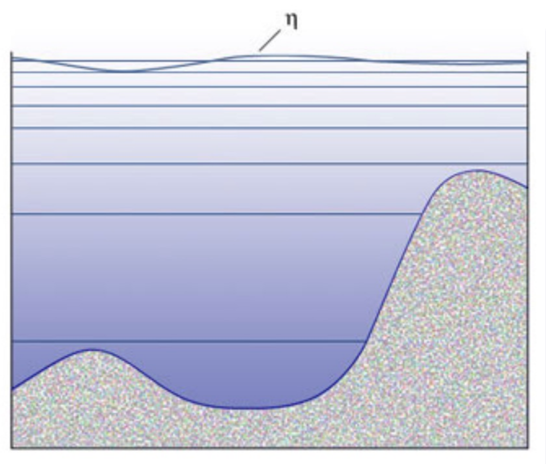

Vertical

Hydrostatic assumption

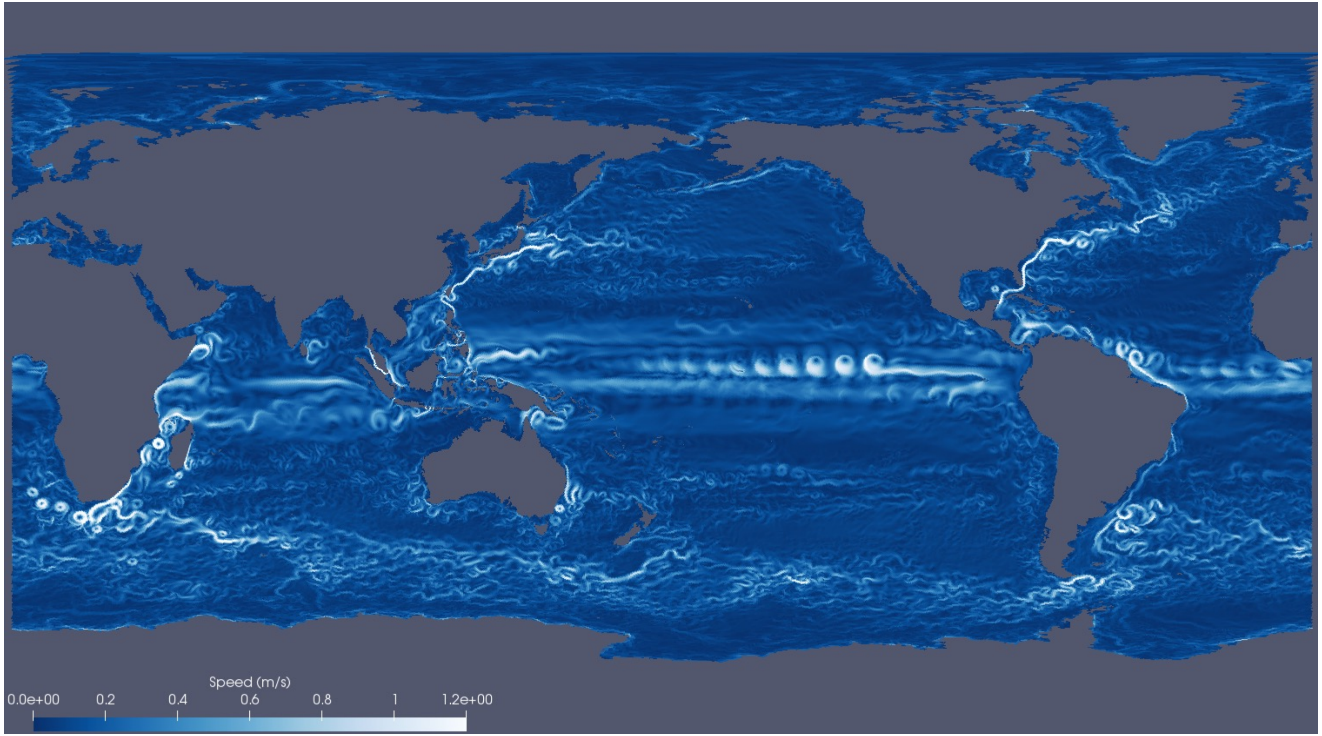

Many modern ocean circulation models adopt the hydrostatic pressure assumption, i.e. they assume that the **pressure at any point in the ocean is due to the weight of the water above it**. For global ocean simulations, where the horizontal scale is considerably larger than the vertical, such an assumption is legitimate.

Los Alamos NATIONAL LABORATORY

Non-hydrostatic model enables new physics...

High-resolution internal wave dynamics not well represented by hydrostatic approximation — **initial verification exercise.**

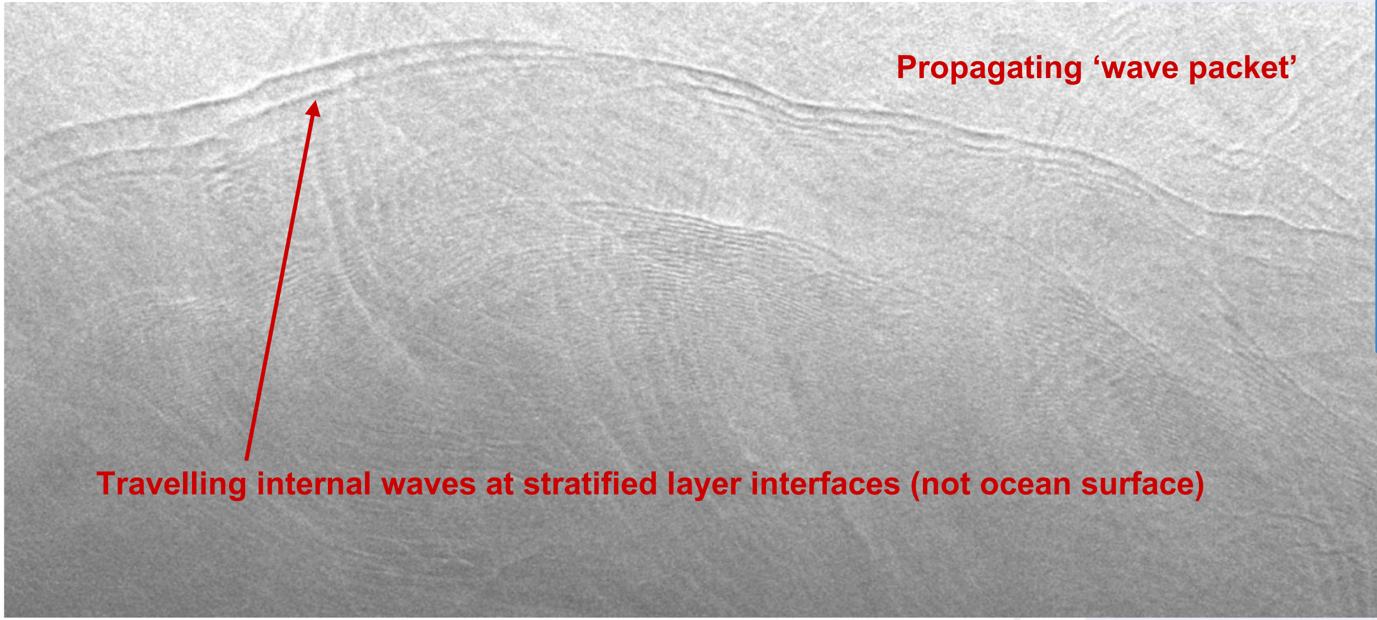

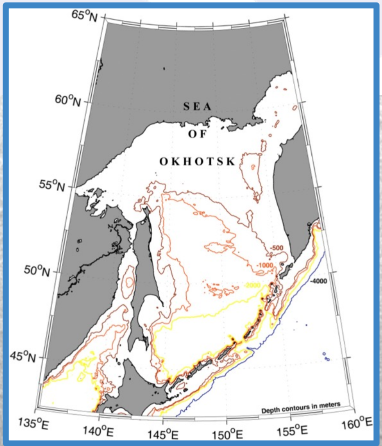

An Atlas of Oceanic Internal Solitary Waves (2004), Office of Naval Research.

Improve MPAS-O: non-hydrostatic formulation

Enhance representation of 3d dynamics via additional vertical momentum/pressure terms.

Hydrostatic

$$\partial_t u + (\mathbf{u}\cdot\nabla)u = -\frac{1}{\rho_0}\nabla_h p' + \dots\,, \tag{1}$$

$$\partial_t h + \nabla\cdot(\mathbf{u}h) = 0\,, \tag{2}$$

$$\nabla\cdot\mathbf{u} = 0\,, \tag{3}$$

$$p = \rho_0 g z + g\int_z \rho(\mathbf{x},t) - \rho_0\,\mathrm{d}z\,. \tag{4}$$

Hydrostatic formulation neglects terms associated with large/fast vertical motion: need nonhydrostatic model for 3d isotropic flows.

Non-hydrostatic

$$\partial_t u + (\mathbf{u}\cdot\nabla)u = -\frac{1}{\rho_0}\nabla_h \boxed{(p' + q)} + \dots\,, \tag{5}$$

$$\boxed{\partial_t w + (\mathbf{u}\cdot\nabla)w = -\frac{1}{\rho_0}\nabla_z\, q + \dots\,,} \tag{6}$$

$$\partial_t h + \nabla\cdot(\mathbf{u}h) = 0\,, \tag{7}$$

$$\nabla\cdot\mathbf{u} = 0\,, \tag{8}$$

$$p = \rho_0 g z + g\int_z \rho(\mathbf{x},t) - \rho_0\,\mathrm{d}z + \boxed{q(\mathbf{x},z,t)}\,. \tag{9}$$

Fringer, Gerritsen, Street (2006): *An unstructured-grid, finite-volume, nonhydrostatic, parallel coastal ocean simulator*, Ocean Modelling.
Vitousek, Fringer (2014): *A nonhydrostatic, isopycnal-coordinate ocean model for internal waves*, Ocean Modelling.

Improve MPAS-O: non-hydrostatic formulation

Non-hydrostatic equations are a coupled elliptic system — use ‘fractional-step’ algorithm:

Forward predictor step:

$$\frac{u^* - u^n}{\Delta t} + (\mathbf{u}^n \cdot \nabla) u^n = -\frac{1}{\rho_0} \nabla_h (p' + q^n) + \dots \, , \tag{10}$$

$$\frac{w^* - w^n}{\Delta t} + (\mathbf{u}^n \cdot \nabla) w^n = -\frac{1}{\rho_0} \nabla_h q^n + \dots \, , \tag{11}$$

‘div-free’ corrector step:

$$\text{set} \quad \nabla \cdot \mathbf{u}^{n+1} = 0 \, , \quad q^{n+1} = q^n + \delta q \tag{12}$$

$$\frac{u^{n+1} - u^*}{\Delta t} = -\frac{1}{\rho_0} \nabla_h \, \delta q \, , \tag{13}$$

$$\frac{w^{n+1} - w^*}{\Delta t} = -\frac{1}{\rho_0} \nabla_z \, \delta q \, . \tag{14}$$

Pressure-correction — 3d elliptic operator:

$$-\frac{1}{\Delta t} (\nabla_h \cdot u^* + \nabla_z \cdot w^*) = -\frac{1}{\rho_0} (\nabla_h \cdot \nabla_h \, \delta q + \nabla_z \cdot \nabla_z \, \delta q) \, , \tag{15}$$

$$\nabla^2 \, \delta q = \rho_0 \frac{1}{\Delta t} \, \nabla \cdot \mathbf{u}^* \tag{16}$$

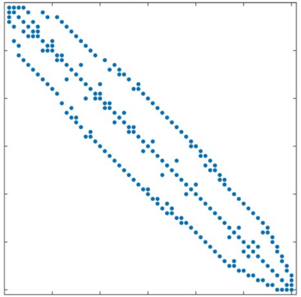

Invert large sparse system of linear equations per time step:

- **Use PETSc library.**
- **Fast approximate soln. using preconditioned iterative Krylov solvers.**

Los Alamos NATIONAL LABORATORY

Fringer, Gerritsen, Street (2006): *An unstructured-grid, finite-volume, nonhydrostatic, parallel coastal ocean simulator*, Ocean Modelling.
Vitousek, Fringer (2014): *A nonhydrostatic, isopycnal-coordinate ocean model for internal waves*, Ocean Modelling.

Improve MPAS-O: non-hydrostatic formulation

- Matrix dimension: # of cells x # of vertical layers, where
  # of cells varies from 1000 to 10M
  # of vertical layers varies from 60 to 100

- CG as solver (KSPCG)

- Block Jacobi as preconditioner (PCBJACOBI) with the number of blocks corresponding to the number of processors

- Other preconditioners tested: PCASM, PCSOR, PCJACOBI

(Dynamic) boundary masking & HPC optimization

Implementation of bottom boundary conditions (land masking) requires careful attention when optimal parallel performance is sought.

Especially critical to support dynamic-in-time vertical layering.

To prevent (expensive) realloc. of the parallel matrix object, we **implement a trailing 'masked block' strategy**. Matrix is maximally alloc.'d at initialization, with 'null' rows added (dynamically) to represent land-mask'd layers under bottom boundary.

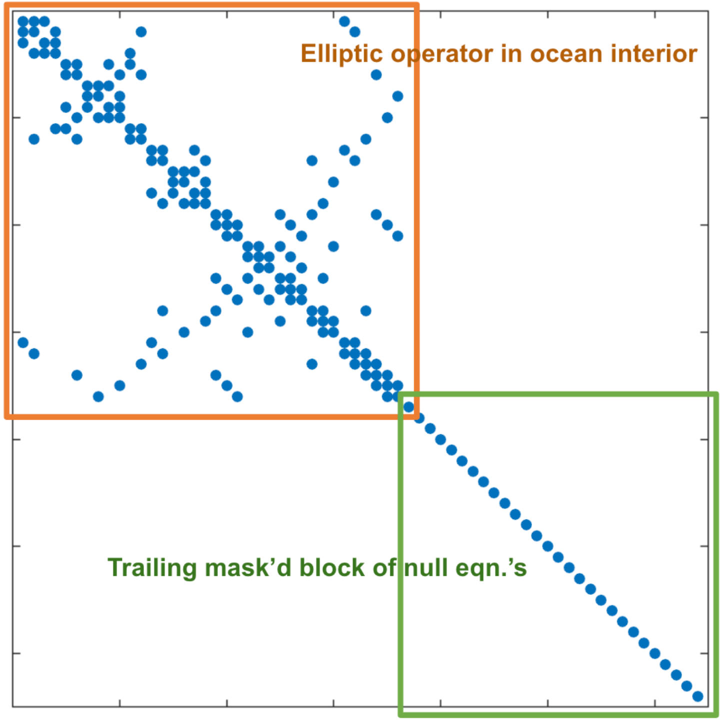

Sparsity pattern of nonhydrostatic elliptic operator, inc. 'masked' block

Los Alamos NATIONAL LABORATORY

Time-steppers in MPAS-O

- 4th order scheme: **RK4**
- 1st order schemes: **split-explicit** and **split-implicit**

The split-explicit and split-implicit algorithms split the governing equations into sub-systems that model the fast (barotropic) and slow (baroclinic) motions separately. The idea is to confine the barotropic mode to a 2D system via vertical averaging, and then to compute the remaining motions explicitly with a long time-step.

Difference between the split-explicit and split-implicit: implicit solver vs explicit sub-cycling for the barotropic mode.

Nonhydrostatic split time-stepper

- Stage 1: Baroclinic velocity (3D)
- Stage 2: Barotropic velocity (2D)
- Stage 3: Update thickness, tracers, density and pressure
  - Forward Euler step for vertical momentum equation.
  - Solution of the elliptic system to get the NH pressure correction.
  - Update of normal velocity, vertical velocity and NH pressure.

Internal Solitary Wave

- Domain: 300km x 2km
  1200 cells, 100 layers

- Density profile:

$$\rho(x,z,t=0) = \rho_0 - \frac{1}{2}\Delta\rho \tanh\left[\frac{2\tanh^{-1}\alpha_s}{\delta_\rho}(z-\xi(x,t=0)+h_1)\right]$$

where

$h_1 = 250$ m, $\alpha_s = 0.99$

$\delta_\rho = 200$ m, $\rho_0 = 1000$ kg m^{-3}, $\Delta\rho/\rho_0 = 0.001.$

$$\xi(x,t=0) = -a_i \exp\left[-\left(\frac{x}{L_\rho}\right)^2\right]$$

$a_i = 250$ m and $L_\rho = 15$ km

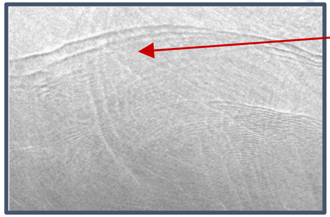

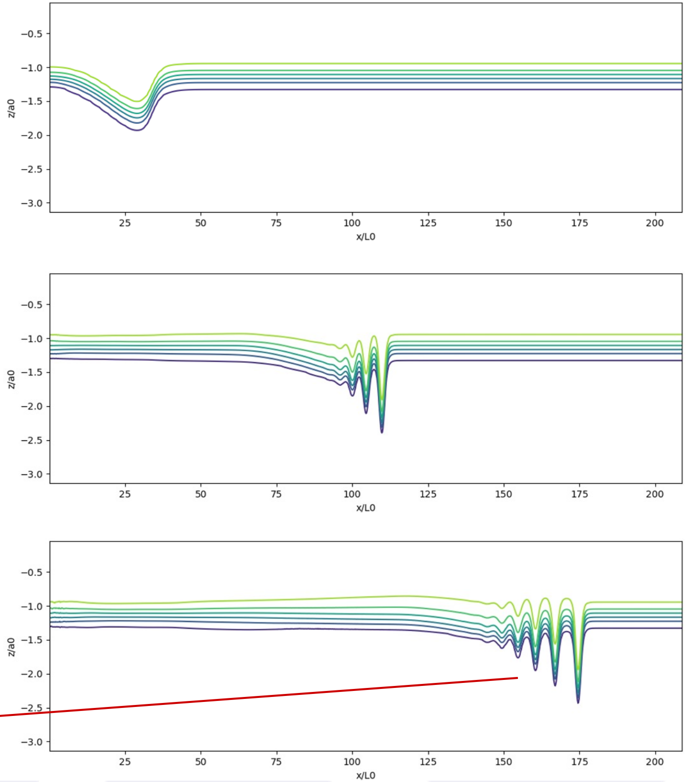

Formation of the internal solitary waves with the nonhydrostatic model after 6h, 24h and 39 h.

Los Alamos NATIONAL LABORATORY

Internal Solitary Wave

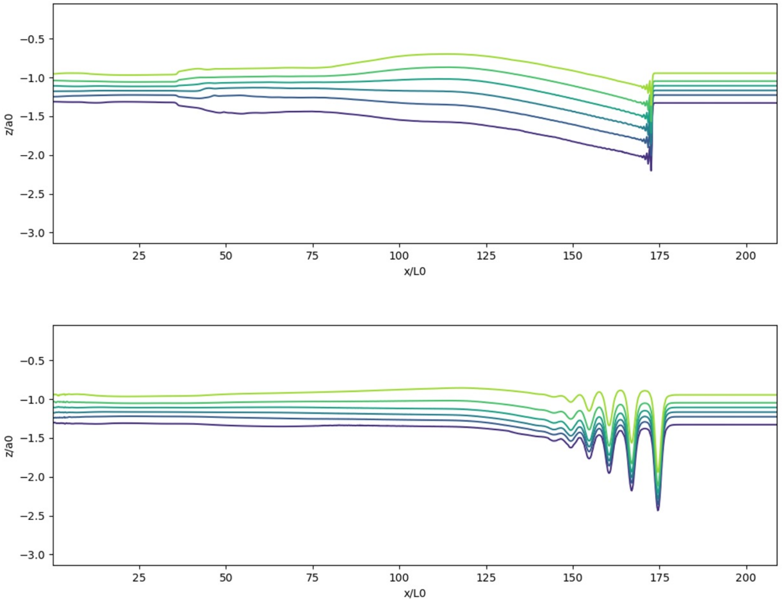

Internal solitary waves train with the hydrostatic model (top) and nonhydrostatic model (bottom) after 39 h.

hydrostatic model fails to capture correct physics at high resolution

In the hydrostatic case, numerical diffusion leads to amplitude loss in the leading solitary-like waves as well as a thickening of the stratification in the lee of the wave train.

Los Alamos NATIONAL LABORATORY

Gravity waves

A **lock-exchange flow** is a prototype problem for gravity waves. The hydrodynamic instability that develops is responsible for the lobe formation at a gravity-current head.

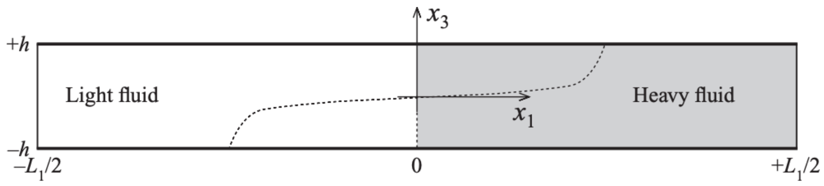

Lock-exchange flow in a channel. The dotted line gives the interface between the two fluids some time after the release (gravity acts in the normal direction x3).

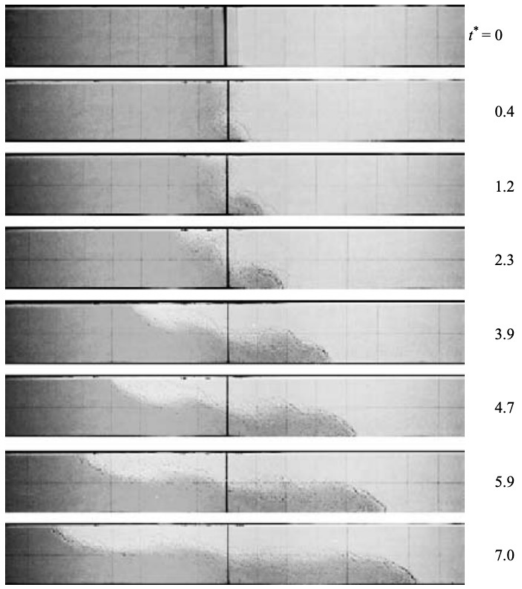

Laboratory lock-exchange flows generated in a plane channel filled with two fluids of different density.

Los Alamos NATIONAL LABORATORY

Nonhydrostatic Lock Exchange Test Case

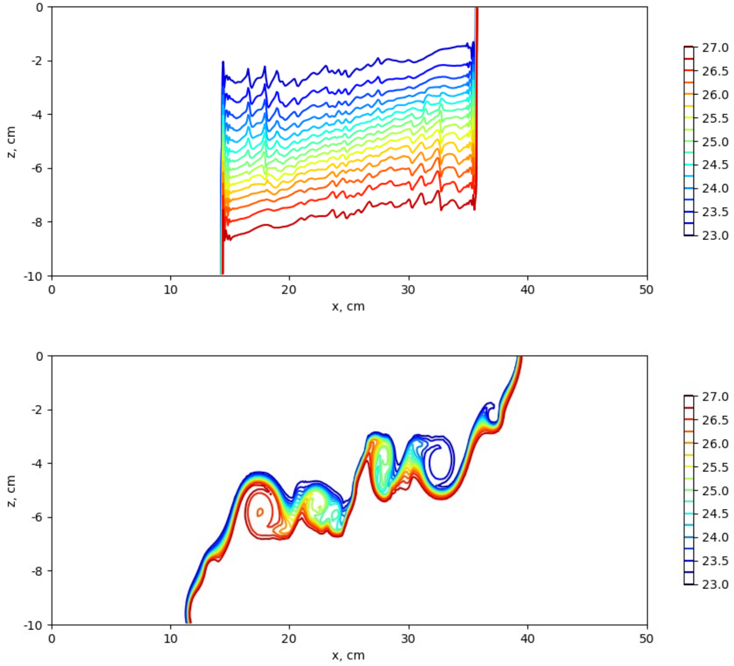

Density profiles at 5s for the nonhydrostatic lock exchange test case.

A Kelvin-Helmholtz instability generates with the nonhydrostatic model which causes vigorous turbulent mixing to develop on the interface between high and low-density water. On the other hand, because of the hydrostatic assumption, in the hydrostatic simulation the density fronts cannot develop in the upper and lower layer.

Plumes

Kelvin–Helmholtz instability is the the main mechanism of mixing in bottom gravity currents and entrainment of **density plumes**.

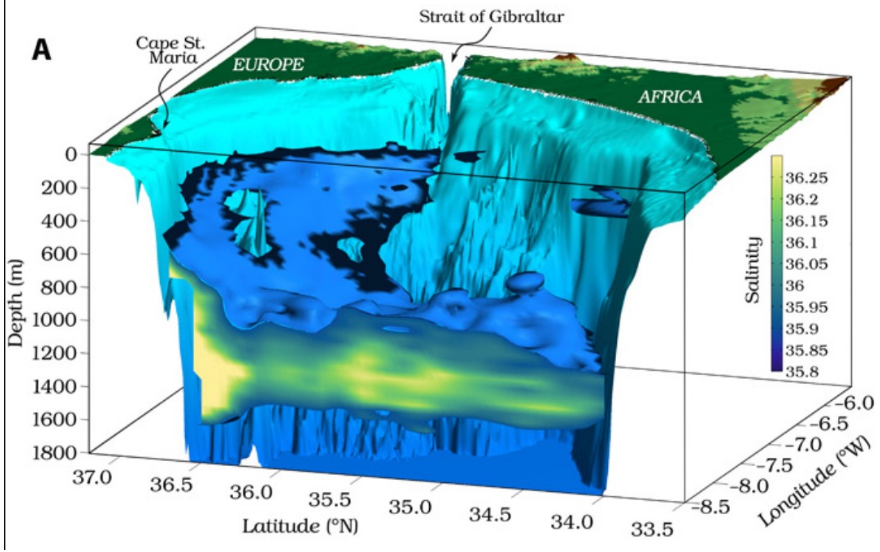

Mediterranean overflow plume: intense evaporation in the Mediterranean Sea produces salty water that sinks to the bottom, flows over the sill in the Strait of Gibraltar, and forms a bottom density current that descends along the continental slope. Observations show that the Mediterranean salinity tongue spreads across the North Atlantic basin at middepths because it is diluted by entrainment of the overlying fresh Atlantic water.

Nonhydrostatic Overflow Test Case

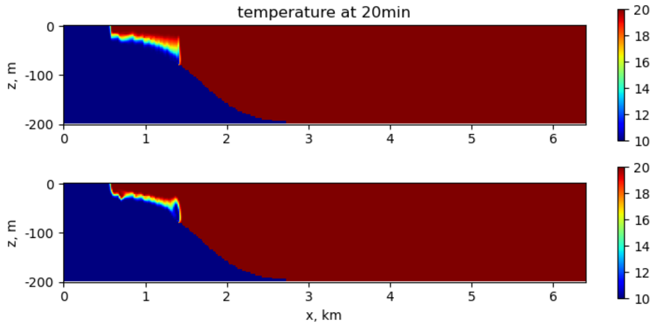

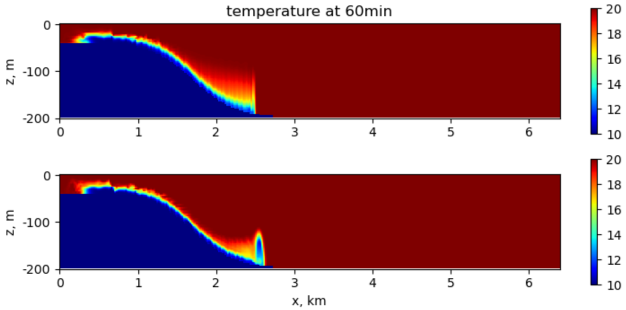

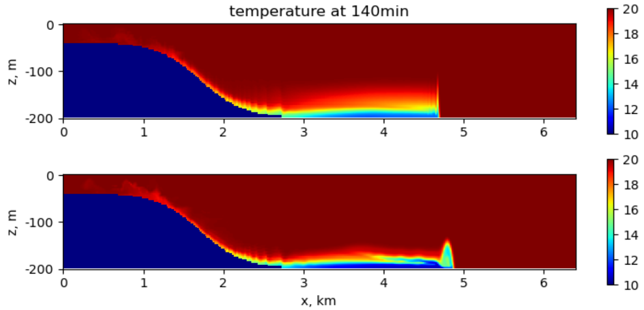

A Kelvin-Helmholtz instability develops in the nonhydrostatic case, leading to entrainment of ambient fluid into a plume. The hydrostatic simulation does not capture the generation of the Kelvin–Helmholtz plume and it also does not correctly capture the speed of the front.

Temperature profiles for the overflow test case at 20, 60 and 140min.

Los Alamos NATIONAL LABORATORY

Nonhydrostatic solver performance

With performance in mind, we have optimized the parallel preconditioning strategy for the nonhydrostatic linear solve.

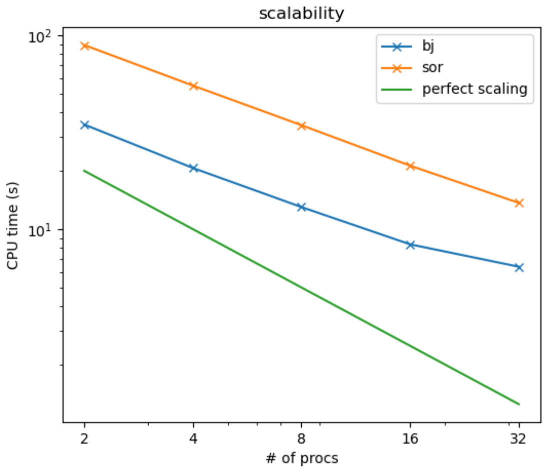

speedup of ~1.6 every time the number of processes doubles

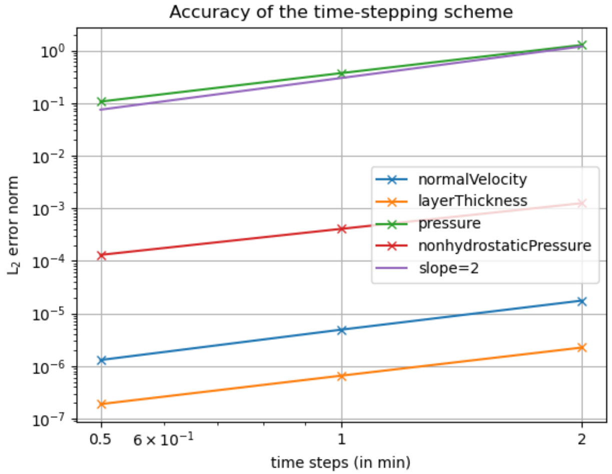

second-order temporal accuracy of the nonhydrostatic formulation

Nonhydrostatic simulations are 3 to 5 times more expensive than the corresponding hydrostatic ones.

Los Alamos NATIONAL LABORATORY

Nonhydrostatic solver performance

Possible improvement in solver performance: time break down for a global ocean simulation run for 1 year with a mesh having 236,000 cells and 60 vertical layers

NH solve -matrix	5658.38591 s
NH solve - rhs	691.49354 s
NH solve - solver	3698.15936 s

The matrix assembly time is longer than the solver time.

Los Alamos NATIONAL LABORATORY

Eddies and nonhydrostatic effects in the wild

Beyond idealized flows, we have developed a high-resolution Gulf of Mexico configuration to **study nonhydrostatic + (sub)mesoscale eddy processes in realistic settings**.

This project is positioned to make a strong impact in this area.

Leveraging MPAS-Ocean variable-resolution capabilities, a hierarchy of regionally-refined (global) domains **from 10km to 2km resolution** has been created.

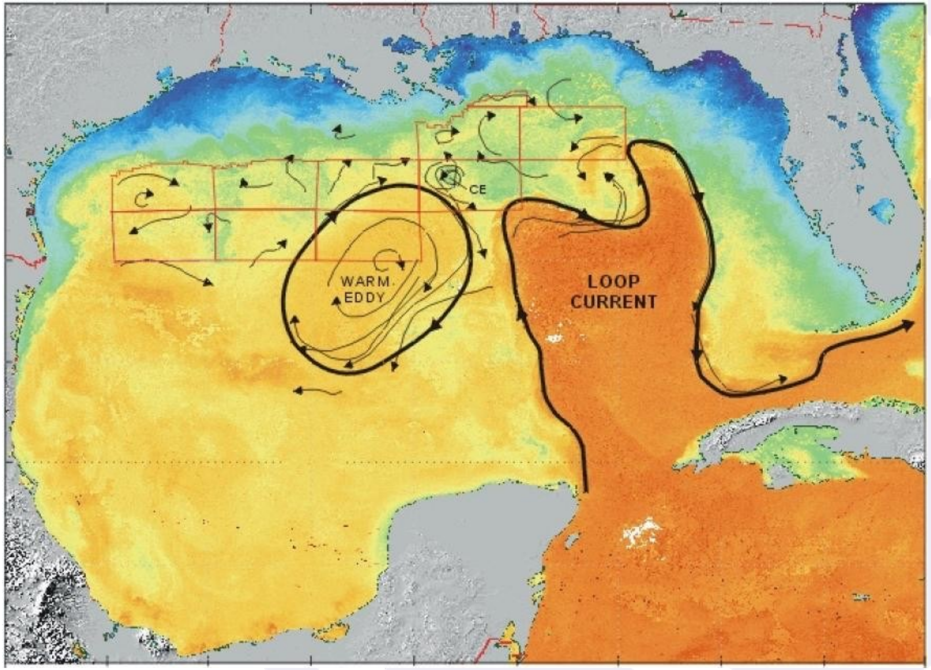

Surface circulation and temperature, courtesy of Horizon Marine

Los Alamos NATIONAL LABORATORY

Gulf of Mexico: submesoscale-permitting dynamics

To capture detailed eddy behaviour, we have developed a new ‘very high-resolution’ config., resolving regionally **down to 2km**.

Compared to the 10km results, the **circulation is significantly stronger**, there is **more eddy activity** overall, and **surface tracer gradients are sharpened**.

In addition to (now well-resolved) mesoscale features, **secondary submesoscale eddies and fronts** are partially resolved.

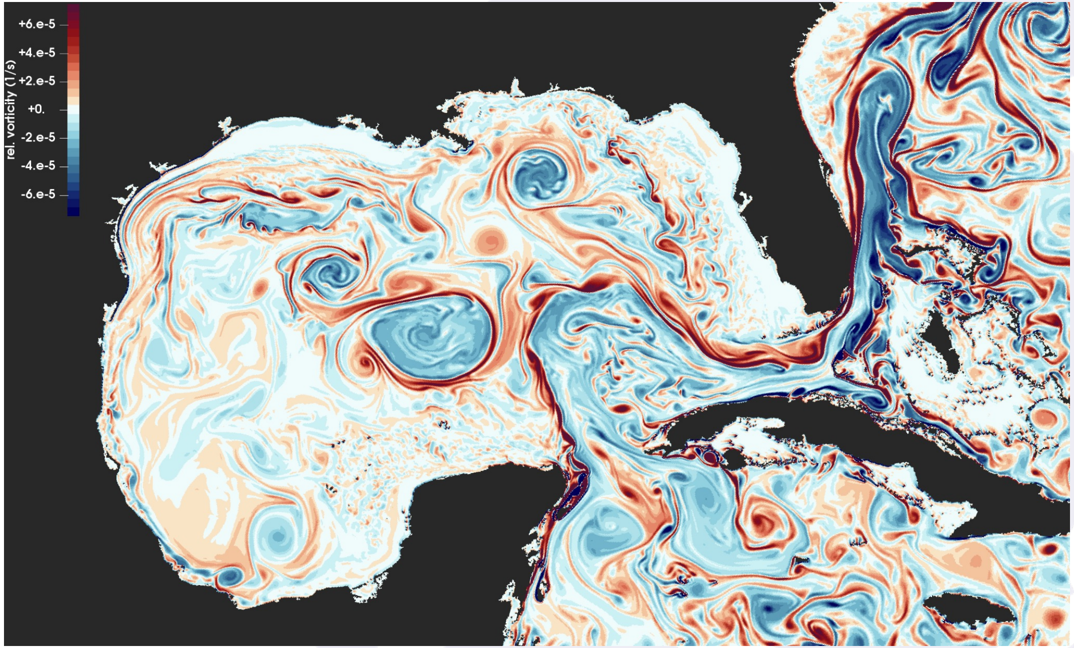

Surface relative vorticity, 30-to-2km ‘submesoscale-permitting’ configuration. Hydrostatic result.

Conclusions

- New nonhydrostatic formulation for MPAS-O that enables new physics.
- Second-order temporal accuracy of the nonhydrostatic formulation.
- Validation on 2D test cases.
- 3 to 5 times more expensive than the hydrostatic model.

➢ Future work: global ocean configurations to better resolve mesoscale and submesoscale features.